Relaxation pathways of the OD stretch fundamental of HOD in liquid H_2O

Beatriz Miguel, José Zúñiga, Alberto Requena, and Adolfo Bastida

Citation: J. Chem. Phys. **145**, 244502 (2016); doi: 10.1063/1.4972128
View online: http://dx.doi.org/10.1063/1.4972128
View Table of Contents: http://aip.scitation.org/toc/jcp/145/24
Published by the American Institute of Physics

Relaxation pathways of the OD stretch fundamental of HOD in liquid H_2O

Beatriz Miguel,[1] José Zúñiga,[2] Alberto Requena,[2] and Adolfo Bastida[2,a)]
[1]*Departamento de Ingeniería Química y Ambiental, Universidad Politécnica de Cartagena, 30203 Cartagena, Spain*
[2]*Departamento de Química Física, Universidad de Murcia, 30100 Murcia, Spain*

(Received 18 October 2016; accepted 30 November 2016; published online 23 December 2016)

The molecular dynamics with quantum transitions method is used to study the vibrational relaxation of the OD stretching mode of HOD dissolved in liquid H_2O water at 303 K. All the vibrational modes of the solute and solvent molecules that participate in the relaxation process are described by quantum mechanics, while the rotational and translational degrees of freedom are treated classically. A modification of the water intramolecular SPC/E (Simple Point Charge/Extended) force field providing vibrational frequencies in solution closer to the experimental values is proposed to analyze the influence of the vibrational energy gaps on the relaxation channels. The relaxation times obtained are in satisfactory agreement with experimental values. The energy transfer during the relaxation process alters significantly the H-bond network around the HOD molecule. The analysis of the vibrational transitions during the relaxation process reveals a complex mechanism which involves the participation of both intra- and intermolecular channels and provides a compromise for the different interpretations of the experimental data reported for this system in recent years. *Published by AIP Publishing.* [http://dx.doi.org/10.1063/1.4972128]

I. INTRODUCTION

Water isotopologues have received much attention in vibrational relaxation studies[1–32] due to the significant changes in their vibrational modes with respect to the parent H_2O molecule, which deeply modify the relaxation dynamics. For example, HOD vibrational modes are better represented using local than normal modes, and the frequencies of the OH and OD stretching bands are significantly shifted, in contrast to the frequencies of the symmetric and antisymmetric stretching bands of liquid H_2O water. This behavior means that HOD is an appropriate molecule in selective laser chemistry.[12,17,24,33–35] In this line, some experimental studies have been performed in an attempt to understand the relaxation process of the OD stretching (ν_{OD}) mode in the HOD/$H_2O_{(l)}$ system. Bakker *et al.*[30,36] carried out a polarization-resolved femtosecond mid-infrared pump-probe spectroscopy study to measure the relaxation time of the ν_{OD} mode in the 1 °C–70 °C temperature range. They elucidated the influence of the temperature on the relative importance of the competitive relaxation pathways through the HOD bending (δ_{HOD}) mode and librations of the solvent, and through the H_2O bending (δ_{H_2O}) mode and librations of the solvent. A relaxation lifetime of 1.90 ps at 303 K was derived using a kinetic model to analyze the experimental data.

Schwarzer *et al.*[29] also performed experimental studies on the ν_{OD} mode relaxation in HOD/$H_2O_{(l)}$ varying the temperatures from 278 to 663 K and the pressure from 1 to 500 bars, in the range of densities $0.28 \leq \rho \leq 1.01$ g/cm^3. The resulting ν_{OD} relaxation lifetime was 1.8 ps at 303 K. The mechanism proposed involved an intermediate state assigned to a nonthermalized state with respect to the nuclear degrees of freedom of the solvent molecules.

More recent experiments, using ultrafast infrared spectroscopy by Tokmakoff's group,[37] found that the lifetime of the OD stretch is similar (~1.45 ps) from 278 K to room temperature and then increases as the temperature rises to 343 K. The authors concluded that there must be multiple competing pathways with different dependencies on temperature. Perakis and Hamm,[38] using two-dimensional infrared spectroscopy, obtained a ν_{OD} relaxation lifetime of 1.35 ps at 293 K. In a recent work, Cho *et al.*[39] performed infrared pump-probe measurements using mid-IR pulses, obtaining a value of 1.79 ps for the ν_{OD} relaxation lifetime at room temperature. They also carried out non-equilibrium molecular dynamics (NEMD) simulations and analyzed the results using the instantaneous spectral density of kinetic energy.[39] The ν_{OD} relaxation was found to proceed with decay times of 0.12 ps (~10%) and 2.42 ps (~90%), resulting in an average lifetime of 0.83 ps.

Previous simulations based on Fermi's golden rule were carried out by Tian[40] using flexible and rigid intramolecular potentials to describe the solvent. The results show a faster energy transfer when using a flexible model of the solvent—5.04 ps versus 19.05 ps—which emphasizes the influence of intramolecular solvent modes as possible energy acceptors during the relaxation. This study concludes that the main relaxation pathway of the ν_{OD} mode is the direct relaxation to the ground state. However, it should be noted that only the δ_{HOD} fundamental was included as an alternative channel, therefore excluding the participation of the HOD bending overtone (δ^2_{HOD}) and the δ_{H_2O} solvent modes.

In this work, we investigate the relaxation dynamics of the ν_{OD} mode of the HOD molecule in liquid H_2O water and the

a)Electronic mail: bastida@um.es

equilibration of the hydrogen bond network in the liquid after the relaxation, using the vibrational Molecular Dynamics with Quantum Transitions (MDQT) method.[41–46] In the present implementation of the MDQT method, both the ν_{OD} mode and all the bending modes of solute and solvent molecules are described quantum mechanically, so the vibration-to-vibration (VV) transitions are treated, naturally allowing us to quantify properly the importance of the competitive intermolecular and intramolecular relaxation channels.

The paper is organized as follows. In Section II we briefly describe the vibrational MDQT method, its application to the HOD/$H_2O_{(l)}$ system, and the computational details of the simulations. Section III presents the numerical results in five subsections: time evolution of the vibrational populations, hop types found in the simulations, vibrational relaxation channels, distribution of the energy during the hops, and effect of the relaxation process in the H-bond network. Section IV summarizes the conclusions drawn in this study.

II. METHODOLOGY

A. The vibrational MDQT method

The Molecular Dynamics with Quantum Transitions (MDQT) method for describing the vibrational relaxation has been extensively described in our previous works,[44,46] so we just outline its main features here. The method is an adaptation of the original treatment developed by Tully[47,48] to describe non-adiabatic electronic transitions. Since it is a hybrid quantum/classical method,[49–56] the system is divided into a classical subsystem, described by time-dependent coordinates and conjugate momenta, and a quantum subsystem characterized by a time-dependent wave function depending on the quantum coordinates. The classical system evolves under the average potential generated by the quantum system. The MDQT method[47] introduces the transition probabilities between the actual quantum state governing the motion of the classical subsystem and the remaining quantum states, and evaluates them in such a way that the fraction of classical trajectories in the *i*th quantum state, the so-called classical population, is equal at all times to the quantum populations. When a hop between two quantum states is invoked, the classical momenta are adjusted to keep the total energy of the system constant.[47,57,58]

The total Hamiltonian for the HOD/$H_2O_{(l)}$ system is defined as in our previous work,[44] using normal coordinates to describe the vibrational motions of each molecule, Euler angles for the rotational motions, and the center of mass vectors for the translational motions. The forces acting on the classical subsystem are calculated by averaging the total Hamiltonian over the wave function of an individual state of the quantum subsystem. The time evolution of the classical subsystem is then propagated using the Hamilton equations. The quantum subsystem, described by the wave function ψ, evolves following the time-dependent Schrödinger equation, which requires evaluating of the couplings between the classical and quantum subsystems.

Usually, the quantum equations of motion are solved by expanding the time-dependent wave function as a linear combination of a given basis set, which can be diabatic or adiabatic. Although an adiabatic basis set is preferable, its use dramatically slows down the hybrid simulations. The alternative is, then, to use diabatic basis sets, which do not depend on the classical coordinates and therefore remain unchanged during the quantum propagation.

We expand the time dependent wavefunction in terms of the following primitive product-type basis set:

$$\psi = d_{gr}\left|f_{gr}\right\rangle + \sum_{i=1}^{N_w} d_i\left|f_i\right\rangle + d_b\left|f_b\right\rangle + d_{st}\left|f_{st}\right\rangle + d_{b,ov}\left|f_{b,ov}\right\rangle, \tag{1}$$

where N_w is the number of H_2O water molecules, d_i are the time-dependent coefficients, $\left|f_{gr}\right\rangle$ describes the ground state of the system

$$\left|f_{gr}\right\rangle = \left|\varphi_{(HOD),gr}\right\rangle \prod_{j=1}^{N_w} \left|\varphi_{(H_2O)_j,gr}\right\rangle, \tag{2}$$

$\left|f_i\right\rangle$ and $\left|f_b\right\rangle$ correspond to the bending excitation of the *i*th H_2O solvent molecule ($\delta_{H_2O,i}$) and the HOD solvent molecule (δ_{HOD}), respectively,

$$\left|f_i\right\rangle = \left|\varphi_{(HOD),gr}\right\rangle \left|\varphi_{(H_2O)_i,ex}\right\rangle \prod_{\substack{j=1 \\ j\neq i}}^{N_w} \left|\varphi_{(H_2O)_j,gr}\right\rangle, \tag{3}$$

$$\left|f_b\right\rangle = \left|\varphi_{(HOD),ex}\right\rangle \prod_{j=1}^{N_w} \left|\varphi_{(H_2O)_j,gr}\right\rangle, \tag{4}$$

$\left|f_{st}\right\rangle$ describes the excitation of the ν_{OD} mode

$$\left|f_{st}\right\rangle = \left|\chi_{(HOD),ex}\right\rangle \prod_{j=1}^{N_w} \left|\varphi_{(H_2O)_j,gr}\right\rangle, \tag{5}$$

and $\left|f_{b,ov}\right\rangle$ accounts for the δ^2_{HOD} overtone excitation of the HOD bending molecule

$$\left|f_{b,ov}\right\rangle = \left|\zeta_{(HOD),ex}\right\rangle \prod_{j=1}^{N_w} \left|\varphi_{(H_2O)_j,gr}\right\rangle. \tag{6}$$

Each of these functions is expressed as products of one-dimensional vibrational wavefunctions in terms of the normal modes of the water molecule as follows:

$$\left|\varphi_{(H_2O)_j,gr}\right\rangle = \left|\varphi_{v=0}(Q_{b,j})\right\rangle \left|\varphi_{v=0}(Q_{ss,j})\right\rangle \left|\varphi_{v=0}(Q_{as,j})\right\rangle, \tag{7}$$

$$\left|\varphi_{(H_2O)_j,ex}\right\rangle = \left|\varphi_{v=1}(Q_{b,j})\right\rangle \left|\varphi_{v=0}(Q_{ss,j})\right\rangle \left|\varphi_{v=0}(Q_{as,j})\right\rangle, \tag{8}$$

$$\left|\varphi_{(HOD),gr}\right\rangle = \left|\varphi_{v=0}(Q_b)\right\rangle \left|\varphi_{v=0}(Q_{OD})\right\rangle \left|\varphi_{v=0}(Q_{OH})\right\rangle, \tag{9}$$

$$\left|\varphi_{(HOD),ex}\right\rangle = \left|\varphi_{v=1}(Q_b)\right\rangle \left|\varphi_{v=0}(Q_{OD})\right\rangle \left|\varphi_{v=0}(Q_{OH})\right\rangle, \tag{10}$$

$$\left|\chi_{(HOD),ex}\right\rangle = \left|\varphi_{v=0}(Q_b)\right\rangle \left|\varphi_{v=1}(Q_{OD})\right\rangle \left|\varphi_{v=0}(Q_{OH})\right\rangle, \tag{11}$$

$$\left|\zeta_{(HOD),ex}\right\rangle = \left|\varphi_{v=2}(Q_b)\right\rangle \left|\varphi_{v=0}(Q_{OD})\right\rangle \left|\varphi_{v=0}(Q_{OH})\right\rangle, \tag{12}$$

which are obtained using the vibrational self-consistent field treatment.[44,46]

We note that the solvent stretching modes and the $\delta^2_{H_2O}$ overtone states are excluded in this treatment because their frequencies are substantially higher (>800 cm^{-1}) than the solute ν_{OD} frequency, so their population during the relaxation process is highly improbable at room temperature

($k_B T \simeq 200$ cm^{-1}). In contrast, the δ^2_{HOD} overtone is only ~400 cm^{-1} higher in frequency than the ν_{OD} mode, so its excitation cannot be ruled out. We use a second-order expansion of the intermolecular potential around the molecular equilibrium geometries and a first-order power expansion of the forces that govern the equations of motion of the classical system, as in our previous studies.[44,46]

B. Computational details

The MDQT simulations were carried out by placing 255 molecules of H_2O and one solute molecule of HOD in the unit cell, giving a total of 255 H_2O bending modes, 1 HOD bending mode, and 1 OD stretching mode to be described quantum mechanically, and 1536 classical translational and rotational coordinates. The unit cell length was appropriately defined to reproduce the experimental water density at 303 K. The Hamilton equations for the translational coordinates were integrated using the leap-frog algorithm,[59] and the classical rotational motions were described using quaternions[59] and propagated using the mid-step implicit leap-frog rotational algorithm proposed by Svanberg.[60] The MDQT simulations were performed including the centrifugal couplings between the rotational and vibrational motions of the individual molecules.

The initial conditions used as starting point in the simulations of the relaxation process came from eight different NVT equilibrium dynamics of the system, taken every 300 ps. The equilibration continued for an extra period of 200 ps, during which initial conditions were taken at time intervals of 2 ps. A time step of 1.5 fs was used in the whole equilibration process and also in the relaxation simulations. The temperature was maintained constant at 303 K during the equilibration by coupling to a thermal bath.[61] The temperature of 303 K was chosen in order to facilitate the comparison with the experimental data.[29,36] The simulations of the relaxation process were performed in the *NVE* ensemble in order to avoid any influence of the velocities scaling on the results. Since the energy transferred from the solute to the solvent (~2500 cm^{-1}) is much smaller than the total kinetic energy of the system, the temperature can also be considered to remain constant during the relaxation period. The quantum wave function was held constant at the $|f_{gr}\rangle$ vibrational ground state during equilibration and set equal to that of the OD stretch fundamental state ($|f_{st}\rangle$) at the beginning of the relaxation process.

In our previous works on the relaxation of both the vibrational bending mode of HOD in liquid D_2O[44] and the vibrational bending mode of H_2O in liquid H_2O,[46] the flexible SPC/E (Simple Point Charge/Extended) potential proposed by Ferguson[62] was used to represent the intra- and intermolecular interactions of the water molecules. In these studies, the only vibrational channels involved in the vibrational relaxation of the bending mode of the initial excited molecule were the bending modes of the solute and the solvent. Although the values of the bending frequencies in the liquid extracted from the simulations were slightly lower than the experimental values, the description of the channels involved in the relaxation was not severely affected by the representation of the potential, since all bending frequencies were similarly shifted. In the present study, we had to consider a larger number of vibrational levels, so the frequency differences between the modes may be important in determining the relative importance of the competing vibrational channels to the relaxation process.

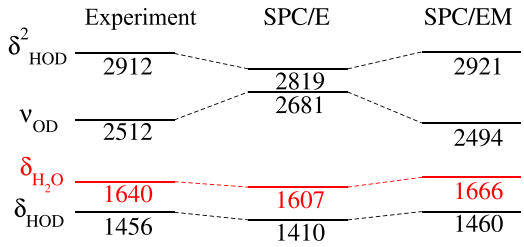

FIG. 1. Vibrational frequencies (in cm^{-1}) of the HOD (black) and H_2O (red) molecules in the HOD/$H_2O_{(l)}$ system. Experimental values are taken from Refs. 37 and 33.

The SPC/E intramolecular water potential[62] is given by

$$U_{intra} = k_l(x - x_e)^2 + k_l\, k_{cubic}(x - x_e)^3 + k_\theta(\theta - \theta_e)^2, \quad (13)$$

where x and θ are the bond length and angle, respectively, and x_e and θ_e are their equilibrium values. The values of the three force constants are k_l = 547.5 kcal mol^{-1} Å^{-2}, k_{cubic} = −1.65 Å^{-1}, and k_θ = 49.9 kcal mol^{-1} rad^{-2}. Figure 1 shows the vibrational energies measured by Tokmakoff *et al.*[37] for HOD/$H_2O_{(l)}$ and by Dlott *et al.*[33] for $H_2O_{(l)}$ as well as those extracted from the MDQT simulations using the SPC/E potential. As observed, the average vibrational frequencies obtained in the simulations underestimate the bending frequencies and significantly overestimate the ν_{OD} ones. In order to reduce these differences, we propose a modification of the original SPC/E potential, referred to as SPC/EM, where the constants k_l and k_θ are readjusted. the new values are k'_l = 473.7 kcal mol^{-1} Å^{-2} and k'_θ = 53.71 kcal mol^{-1} rad^{-2}. As shown in Figure 1, using the SPC/EM potential in the MDQT simulations gives much better agreement between the calculated frequencies and experiment than that provided by the original SPC/E potential, and leads to an increase in the energy gap between δ^2_{HOD} and ν_{OD} modes and a decrease of the gaps between ν_{OD} and both δ_{HOD} and δ_{H_2O} bending modes. we have performed the MDQT simulations using both potentials in order to quantify the importance of these energy differences on the relaxation pathways.

III. RESULTS

A. Classical and quantum populations

The time evolution of the classical populations of the states involved in the vibrational relaxation of the ν_{OD} mode is presented in Figure 2. The initial state population decreases during the relaxation, tending to zero at long times, and the ground state population increases continuously towards one. Since the energies of the excited vibrational levels involved in the relaxation process are much higher than the thermal energy of 303 K (see Figure 1), we can expect that only the ground state will be populated at the equilibrium according to the Boltzmann distribution. As usual, the disagreement between classical and quantum populations (not shown) appears in the first steps of the simulation and is maintained at long times, since the trajectories decaying to the ground state remain

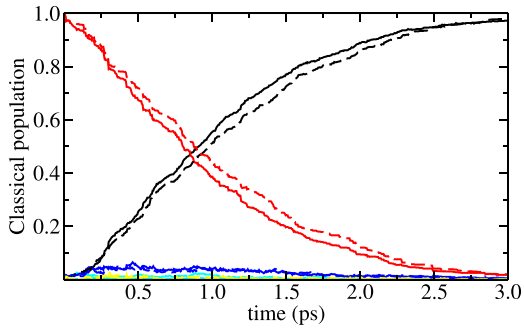

FIG. 2. Time evolution of the classical populations during the ν_{OD} mode relaxation calculated using the MDQT method with the SPC/E potential (solid lines) and the SPC/EM potential (dashed lines), at 303 K. Populations correspond to the ν_{OD} (red), ground (black), δ^2_{HOD} (cyan), δ_{HOD} (blue), and δ_{H_2O} (yellow) states as described in Section II A.

trapped in it because most of the transitions from the ground state to the excited states are energetically forbidden.[47,63] For this reason, the classical populations have shorter lifetimes and correctly reproduce the thermodynamical equilibrium populations of the states at longer times.[44,46] We should note also that there is a smooth recurrence at ~175 fs during the decay of the initial state quantum population which is not clearly visible in the classical populations shown in Figure 2. This recurrence has been previously found experimentally by Tokmakoff *et al.*[64] at 170 fs in their study of the HOD/D_2O system, suggesting that it may arise from the oscillatory motion of the H-bond intermolecular coordinate.

As shown in Figure 2, the decay of the ν_{OD} population obtained with the SPC/E potential is only slightly faster than that obtained with the SPC/EM potential. Among the intermediate vibrational states involved in the relaxation, the δ_{HOD} mode reaches the highest population, ~7%, while the populations of the δ_{H_2O} and δ^2_{HOD} modes do not exceed 4% and 3%, respectively, with the SPC/E potential. In the dynamics with the SPC/EM potential, the maximum population of the δ^2_{HOD} overtone is one third lower than that obtained using the SPC/E potential and the population of the δ_{H_2O} mode is almost double.

The ν_{OD} relaxation lifetime in the MDQT dynamics has been defined as the time taken for the population to decrease to $1/e$ and results in 1.03 ps for the SPC/E potential and only a slightly higher value—1.18 ps—for the SPC/EM potential. Both lifetimes are shorter than the experimental values obtained by several other techniques, 1.90 ps at 303 K by Smit and Bakker,[36] 1.8 ps at 303 K by Schwarzer *et al.*,[29] 1.6 ps at 323 K by Tokmakoff's group,[37] 1.35 ps at 293 K by Perakis and Hamm,[38] and 1.794 ps by Cho *et al.*[39] at room temperature. However, we recall that the MDQT simulations do not include any adjustable parameter (except for the scaling of the force constants in the SPC/EM potential) so we can consider the agreement with the experimental findings satisfactory.

In the molecular dynamics study based on the Fermi's golden rule performed by Tian,[40] the resulting ν_{OD} relaxation lifetime was 5.04 ps. While the author used a different intramolecular potential from that used in this work, it is expected that the description of the vibrational states involved in the relaxation of the ν_{OD} stretching mode will not change much because such states have low energies and practically behave harmonically. Compared with these pure classical results, the present MDQT simulations reduce the lifetime by a factor of ~5, placing the relaxation lifetime much closer to the experimental data. This decrease demonstrates the importance of the quantum description of the vibrational modes of the solvent molecules, as was already shown in our works on the relaxation of the bending mode in the HOD/$D_2O_{(l)}$ and $H_2O_{(l)}$[46,65] systems.

A recent NEMD study by Cho *et al.*[39] provided an average ν_{OD} relaxation lifetime of 0.83 ps. In this case the relaxation process is accelerated due to uphill energy transfer to both the OH stretch mode of the HOD molecule and the stretching modes of the solvent H_2O molecules, which is an unphysical effect resulting from the classical description of the vibrations of the system.

B. Hop types

The MDQT method provides detailed information on the hops between the vibrational energy levels taking place during the relaxation process and allows therefore to quantify the relative contributions of both the intramolecular channels corresponding to transitions between vibrational states of HOD and the intermolecular channels involved in the energy transfer between the HOD solute molecule and the H_2O solvent molecules. We have considered 19 types of hops during the relaxation, and these are presented in Table I. In our previous studies on the relaxation of the bending mode in the HOD/$D_2O_{(l)}$[44] and $H_2O_{(l)}$[46] systems, the number of hop types, 7, was substantially smaller due to the comparatively lower energy of the initial excited state. As observed in Table I, all direct hops are accompanied by the corresponding reverse

TABLE I. Average number of hops per trajectory and the vibrational energy transferred (ΔE_{vib} = E_{vib} (final state)—E_{vib} (initial state)) (in cm^{-1}) obtained in the MDQT simulations during the relaxation of the ν_{OD} mode.

		Number		ΔE_{vib}	
	Hop	SPC/E	SPC/EM	SPC/E	SPC/EM
1	$\nu_{OD} \rightarrow$ ground	0.200	0.186	−2681	−2493
2	Ground $\rightarrow \nu_{OD}$	0	0	2681	2493
3	$\nu_{OD} \rightarrow \delta^2_{HOD}$	0.292	0.078	123	404
4	$\delta^2_{HOD} \rightarrow \nu_{OD}$	0.080	0.016	−136	−420
5	$\nu_{OD} \rightarrow \delta_{HOD}$	0.478	0.524	−1274	−1035
6	$\delta_{HOD} \rightarrow \nu_{OD}$	0.066	0.069	1280	1039
7	$\nu_{OD} \rightarrow \delta_{H_2O}$	0.181	0.294	−1072	−830
8	$\delta_{H_2O} \rightarrow \nu_{OD}$	0.002	0.005	1090	824
9	$\delta^2_{HOD} \rightarrow$ ground	0	0	−2752	−2683
10	Ground $\rightarrow \delta^2_{HOD}$	0	0	2752	2683
11	$\delta^2_{HOD} \rightarrow \delta_{HOD}$	0.177	0.045	−1403	−1459
12	$\delta_{HOD} \rightarrow \delta^2_{HOD}$	0.009	0.001	1399	1469
13	$\delta_{HOD} \rightarrow$ ground	0.614	0.519	−1403	−1457
14	Ground $\rightarrow \delta_{HOD}$	0.040	0.019	1409	1451
15	$\delta_{HOD} \rightarrow \delta_{H_2O}$	0.024	0.029	196	200
16	$\delta_{H_2O} \rightarrow \delta_{HOD}$	0.021	0.031	−201	−215
17	$\delta_{H_2O}/\delta'_{H_2O} \rightarrow$ ground	0.260	0.365	−1604	−1664
18	Ground $\rightarrow \delta_{H_2O}$	0.087	0.079	1603	1666
19	$\delta_{H_2O} \rightarrow \delta'_{H_2O}$	0.050	0.095	0	0
	Total	2.59	2.35		

hops, with their initial and final vibrational states exchanged, except for the hop between bending states of two different H_2O solvent molecules.

For the sake of clarity, in Figure 3 we plot the direct hops gathered in groups which share the initial vibrational state of the transition. The first of the five groups proposed (blue arrows) corresponds to hops 1, 3, 5, and 7 which, respectively, represent the relaxation of the initially excited ν_{OD} stretching mode to the ground state, the intramolecular VV transfers to the δ^2_{HOD} overtone mode and to the δ_{HOD} bending mode, and the intermolecular VV transfer to the δ_{H_2O} bending mode of a solvent molecule. As shown in Table I, hop 5, corresponding to the $\nu_{OD} \rightarrow \delta_{HOD}$ transition, is the most frequent in the simulation, with a value of 0.48 hops per trajectory for the SPC/E potential, while hops 1, 3, and 7 occur with lower percentages, 0.20, 0.29, and 0.18, respectively.

The second group of hops (red arrows) describes the relaxation of the δ^2_{HOD} bending overtone and includes hops 9 and 11 corresponding to the transition to the ground state and the intramolecular VV transfer to the δ_{HOD} bending mode. Intermolecular VV transfer from the δ^2_{HOD} overtone to the δ_{H_2O} bending mode of a solvent molecule is not considered since the coupling between the these two states depends on the cubic terms of the potential, which are not included in the potential expansion due to their much lower values compared to the quadratic terms. As has been seen, no direct relaxation of the δ^2_{HOD} overtone to the ground state is observed, so the intramolecular VV transfer to the δ_{HOD} bending mode is the only existing channel.

The relaxation channels of the δ_{HOD} mode are collected in the third group of hops (yellow arrows). Here, hop 13, corresponding to the relaxation to the ground state, is strongly favored over hop 15 which describes the intermolecular VV transfer to a δ_{H_2O} mode with 0.61 hops versus 0.024 hops.

Hop 17 (magenta arrows) includes the relaxation of the δ_{H_2O} solvent modes to the ground state while hop 19 (magenta arrow) corresponds to the resonant intramolecular VV transfer between the δ_{H_2O} modes of two different solvent molecules. This process only accounts for 0.05 hops per trajectory.

The reverse hops correspond to the even numbers, from 2 to 18. These hops allow us to evaluate the reversibility of the hops along the dynamic. In general, we observe that if

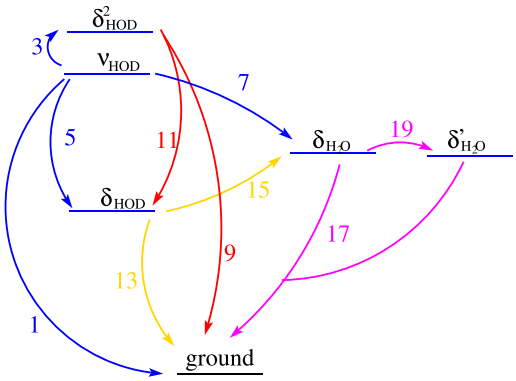

FIG. 3. Different types of hops considered in the vibrational relaxation of the ν_{OD} mode. Hops are grouped according to the initial vibrational state: ν_{OD} (blue), δ^2_{HOD} (red), δ_{HOD} (yellow), and δ_{H_2O} (magenta).

the energy difference between the two vibrational levels is high enough compared to the thermal energy at the working temperature, the hops are practically irreversible. When the energy difference is similar to the thermal energy, see, for instance, hops 3-4 and 15-16, the reversibility of the hop is, in general, enhanced. A particular case corresponds to hops 17-18 where the reversibility is strongly favored by the high number of δ_{H_2O} solvent molecules of the system.

The changes in the number of hops obtained when using the SPC/EM potential instead of the SPC/E potential are directly related with the modifications of the energy gaps. For example, in hop 3 the energy gap increases from 123 cm^{-1} to 404 cm^{-1} and the relaxation of the ν_{OD} mode through the δ^2_{HOD} overtone consequently decreases in importance, from 0.29 to 0.08 hops per trajectory. In contrast, the number of hops per trajectory for the $\nu_{OD} \rightarrow \delta_{H_2O}$ transition increases from 0.181 to 0.294, since the energy gap between the modes is reduced from −1072 to −830 cm^{-1}.

The average total number of hops per trajectory obtained in the simulations using the SPC/E potential is 2.59 and decreases slightly to 2.35 for the SPC/EM potential. This difference is mainly due to the decrease of the type 3 of hops ($\nu_{OD} \rightarrow \delta^2_{HOD}$), which also provokes the decrease of the value for hop 11 ($\delta^2_{HOD} \rightarrow \delta_{HOD}$).

The number of hops considered in the dynamics and their relative magnitudes allow us to infer that the vibrational relaxation of the ν_{OD} mode of HOD involves a complex mechanism in which there is no dominant channel and that several competitive pathways contribute to the overall process. This aspect will be discussed in more detail in Subsection III C.

C. Vibrational relaxation channels

We now evaluate the net flows of vibrational populations during the relaxation of the ν_{OD} mode by considering the contribution of the direct and reverse transitions included in Table I. The percentages of molecules following each relaxation channel are shown in Figure 4.

We start our discussion with the results obtained using the SPC/E potential. We note that in the first stage of the ν_{OD} mode relaxation, the intramolecular transfers of energy to the δ^2_{HOD} overtone, the δ_{HOD} mode, and the ground state are favored, since they account for 82.4% of the relaxation, while the relaxation through intermolecular transfer to the δ_{H_2O} bending mode only contributes 17.6%. The greatest contribution to the intramolecular ν_{OD} relaxation comes from the δ_{HOD} bending mode, a pathway followed by 41.2% of the molecules, compared to 21.2% of the molecules relaxing through the δ^2_{HOD} bending overtone and 20% relaxing directly to the ground state.

The relaxation of the ν_{OD} mode populates the δ^2_{HOD}, δ_{HOD}, and δ_{H_2O} modes, which subsequently relax in a second step. Vibrational relaxation of the δ^2_{HOD} bending overtone to the ground state occurs through the δ_{HOD} bending mode as intermediate. The relaxation of the δ_{H_2O} bending mode mostly occurs to the ground state by transferring the vibrational energy into rotational and translational modes of the system, with a small intermolecular VV transfer contribution to the δ'_{H_2O} bending mode of another water molecule. This VV intermolecular energy transfer between the bending modes of

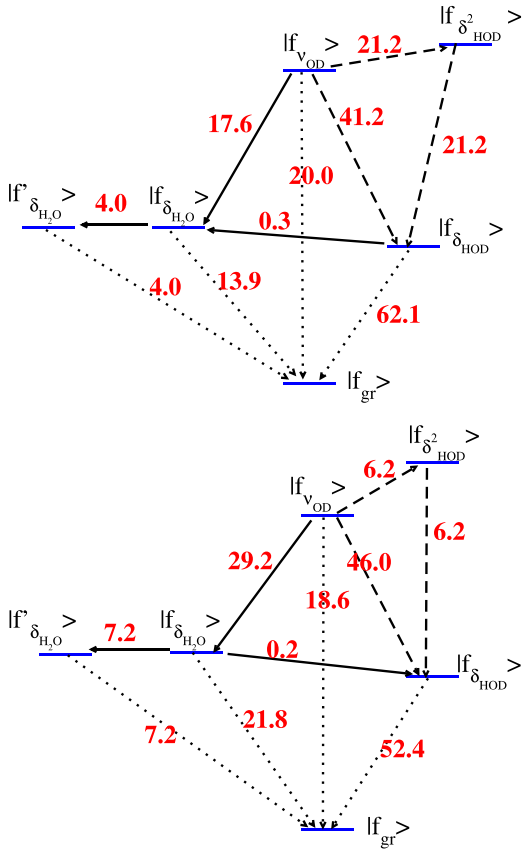

FIG. 4. Importance of vibrational channels (in %) that contribute to the ν_{OD} mode relaxation in the HOD/$H_2O_{(l)}$ system obtained using the SPC/E potential (top) and the SPC/EM potential (bottom). The dashed lines correspond to intramolecular VV transitions of the HOD solute molecule, dotted lines to direct relaxation to the ground state, and the solid lines to VV intermolecular transitions. Vibrational levels are placed according to their relative frequencies shown in Figure 1.

H_2O molecules was previously found in the δ_{H_2O} relaxation dynamics in $H_2O_{(l)}$,[46] where it was the main channel. The difference in importance of this VV intermolecular channel is likely due to the fact that, after the ν_{OD} mode relaxation, an excitation of the rotational and translational modes of the system follows that affects the subsequent energy transfers, whereas the vibrational relaxation of the δ_{H_2O} mode in $H_2O_{(l)}$ is produced at equilibrium conditions.

Overall, we note that 62.1% of the molecules reach the ground level following the relaxation to the δ_{HOD} bending mode, 20% of them suffer a direct relaxation of the ν_{OD} mode, and 17.9% relax through the δ_{H_2O} bending mode of the solvent molecules. Therefore, only one of every six molecules relaxes through an intermolecular channel while the remaining ones follow an Intramolecular Vibrational Redistribution (IVR) process.

When the SPC/EM potential is used in the MDQT dynamics, we obtain that the transfer of one vibrational quantum from the stretching mode, ν_{OD}, to the δ^2_{HOD} overtone is clearly disfavored, decreasing from 21.2% to 6.2% due to the increase in the corresponding energy gap (see Table I). In contrast, the intramolecular VV transfer to the δ_{HOD} mode increases from 41.2% to 46.0% and the intermolecular VV to the δ_{H_2O} mode increases from 17.6% to 29.1%. In both cases, the energy gap between the ν_{OD} mode and the bending modes decreases when the SPC/EM potential is used from 1274 cm^{-1} to 1035 cm^{-1} for the δ_{HOD} mode and from 1072 to 830 cm^{-1} for the δ_{H_2O} mode, due to the change in frequency of the ν_{OD} mode in the SPC/EM potential. The decrease of these energy gaps favors these transitions in the SPC/EM potential. The importance of the channel associated to the direct energy transfer from the ν_{OD} stretching mode to the ground state is only slightly affected by the potential description—being 20.0% with the SPC/E potential and 18.6% with the SPC/EM—since the energy gap only decreases to ~7%.

We find in the literature that different mechanisms have been proposed to describe the vibrational relaxation of the ν_{OD} mode in HOD/$H_2O_{(l)}$. Bakker *et al.*[30,36] propose three possible mechanisms for the relaxation of the ν_{OD} stretching mode, a first channel including relaxation to the δ_{HOD} mode and librations of the solvent, a second channel involving the excitation of the δ_{H_2O} mode and librations of the solvent, and a third channel corresponding to the direct energy transfer to the hydrogen bonds. They excluded the relaxation mechanism through the δ^2_{HOD} overtone and suggest that the first two channels are the most important in the relaxation, with one or the other dominating depending on the temperature, while the third one can be excluded as a significant relaxation channel. The relaxation to the δ_{HOD} mode dominates in the ice phase while relaxation to the δ_{H_2O} mode is more important in the water phase. On the other hand, in the experimental work by Schwarzer *et al.*[29] a difference is found between the time taken for the ν_{OD} mode to relax and the time taken for ground state to be populated, so the authors conclude that there must be an intermediate state corresponding to a state which is not in thermal equilibrium. They suggest that the ν_{OD} mode mainly relaxes to the ground state, avoiding the δ_{HOD} mode, and assign the intermediate to a state associated with the excitation of rotational and translational of degrees freedom of the system which relaxes by reorganizing the network of hydrogen bonds.

Molecular dynamics simulations based on Fermi's golden rule[40] indicate that the main relaxation channel is $\nu_{OD} \rightarrow \delta_{HOD} \rightarrow$ ground. However, in this study, neither is the δ^2_{HOD} overtone included nor were the δ_{H_2O} bending modes of solvent molecules considered.

Recent NEMD simulations[39] state the participation of the δ_{HOD} and δ_{H_2O} modes as intermediates during the ν_{OD} relaxation, in agreement with the MDQT results. However, it is difficult to make a more detailed comparison since the classical description of the vibrational modes greatly complicates the quantification of the energy flows and because of the presence of high frequency modes that receive significant amounts of energy contrary to the physical evidence.

Overall, the experimental and theoretical studies do not agree about the ν_{OD} relaxation pathways since they identify different intermediate states. The MDQT simulations provide a simple explanation to these apparently contradictory results by proposing that three intermediate states, δ^2_{HOD}, δ_{HOD}, and δ_{H_2O}, contribute significantly to the relaxation.

D. Distribution of energy in hops

An interesting question is how the energy is redistributed from the vibrational quantum states to the classical rotational and translational degrees of freedom when a hop occurs. In

TABLE II. Average number of hops per trajectory and changes in the vibrational (ΔE_{vib}), rotational (ΔE_{rot}), and translational (ΔE_{tr}) energies (in cm^{-1}) for molecules involved in the transition and the solvent, for the hops from the initially excited ν_{OD} mode. Superscripts I and F refer to the molecule that loses or gains, respectively, a vibrational quantum in the hop. The superscript sol represents molecules whose vibrational state $v = 0$ does not change in the hops. For each type of hop, two sets of results are presented: those obtained in the simulations with the SPC/E potential (first row) and with the SPC/EM potential (second row).

Hop		Number	ΔE_{vib}	ΔE^I_{rot}	ΔE^I_{tr}	ΔE^F_{rot}	ΔE^F_{tr}	ΔE^{sol}_{rot}	ΔE^{sol}_{tr}
1	$\nu_{OD} \rightarrow$ ground	0.200	−2680.9	791.4	448.5	...	...	965.1	476.9
		0.186	−2493.3	745.7	419.5	...	...	889.1	440.1
3	$\nu_{OD} >\!\!\rightarrow \delta^2_{HOD}$	0.292	122.8	−0.5	−0.0	...	...	−116.1	−10.4
		0.078	404.2	0.6	−0.0	...	...	−374.5	−34.8
5	$\nu_{OD} >\!\!\rightarrow \delta_{HOD}$	0.478	−1273.7	45.3	2.9	...	...	1222.2	1.6
		0.524	−1035.3	36.8	2.5	...	...	993.3	1.2
7	$\nu_{OD} >\!\!\rightarrow \delta_{H_2O}$	0.181	−1072.1	191.8	−0.4	67.6	1.7	726.0	86.6
		0.294	−829.6	149.5	−0.3	48.8	1.3	562.8	64.7

Table II we include the vibrational, rotational, and translational energies exchanged during the relaxation of the ν_{OD} mode. These quantities are detailed separately for molecules that gain or lose a vibrational quantum in some of their vibrational modes, while the remaining molecules are labeled as solvent. Positive values in Table II indicate that, after adjustment of the classical momenta in the hop, the molecules increase their energy, while negative values indicate the opposite.

We observe that the energy transfer to the rotational degrees of freedom is favored over the transfer to the translational ones. This result has already been observed in the classical[66] and MDQT[44] simulations of the relaxation of the δ_{HOD} mode of the $HOD/D_2O_{(l)}$ systems and it was attributed to rovibrational couplings. The direct relaxation of the ν_{OD} stretching mode to the ground state involves the biggest amount of energy, which is redistributed into the rotational (21.5%) and the translational (16.7%) degrees of freedom of the HOD molecule, and the rotational (36.0%) and the translational (17.8%) degrees of freedom of the solvent molecules. In the transition to the δ^2_{HOD} mode, which involves the smallest energy exchange, the translational and rotational energies of the HOD molecule barely change, and the solvent molecules receive the energy from the vibrational transition. We also note that when the relaxation occurs through energy transfer to solute (hop 3) or to solvent (hop 7) bending modes, the largest amount of energy goes to the rotational degrees of freedom of the environmental molecules.

Overall, there are no noticeable differences between the energy distribution results obtained using the SPC/E and SPC/EM potentials, although the magnitude of the energy changes modifies according to the modifications of the energy gaps.

E. Effect of the vibrational relaxation on the H-bond structure

The vibrational energy released in relaxation of a vibrational mode which is not transferred to a different vibrational mode is redistributed among the remaining translational and rotational degrees of freedom of the solute and solvent molecules. This energy transfer produces an alteration of the structural environment of the molecule that loses the vibrational energy, thus modifying the structure of hydrogen bonds and the surrounding solvation shells. The distribution of this excess energy will vary over the time until the system returns to its thermal equilibrium. We have considered here the hops corresponding to the direct relaxation of the OD mode to the ground state (hop type 1), which accounts for the highest energy transfer into the solvent.

To follow the time evolution of this reorganization, we define the hydrogen bond as in our previous work,[44,67] that is, by classifying every intermolecular H···O/D···O pair as H-bonded if the H···O/D···O intermolecular distance is less than the position of the first minimum of the radial distribution function $g_{OH}(r)$ at 2.41 Å. Figure 5 shows the temporal evolution of the difference between the number of H-bonds after a hop type 1 and the number of hydrogen bonds in thermal equilibrium for the solute molecule. Previous results obtained using the same methodology for the relaxation of the δ_{H_2O} mode in $H_2O_{(l)}$[46] and the δ_{HOD} mode in $HOD/D_2O_{(l)}$[44] are also included for comparison. The number of H-bonds at equilibrium is 3.77 for $HOD/H_2O_{(l)}$ at 303 K and $HOD/D_2O_{(l)}$ at 298 K and 3.78 for H_2O at 295 K.

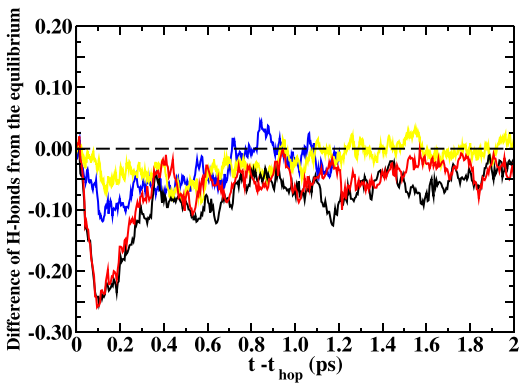

FIG. 5. Temporal evolution of the average number of hydrogen bonds with respect to their equilibrium values during the relaxation of the ν_{OD} mode to the ground state in the $HOD/H_2O_{(l)}$ system obtained using the SPC/E (black line) and the SPC/EM (red line) potentials. Also shown are the results corresponding to the relaxation of the δ_{H_2O} mode in $H_2O(l)$[46] (blue line) and the δ_{HOD} mode in $HOD/D_2O_{(l)}$[44] (yellow line).

As observed, the energy released during the relaxation of the ν_{OD} mode significantly alters the H-bond network, with the number of H-bonds decreasing by ~−0.25 during the first 100 fs. This decrease is more important than that previously found during the relaxation of the bending mode in the $H_2O_{(l)}$ and $HOD/H_2O_{(l)}$ systems. This is due to the higher amount of energy transferred during the relaxation of the ν_{OD} mode (2681 cm^{-1}), as compared to the relaxation of the δ_{HOD} (1607 cm^{-1}) and the δ_{HOD} (1410 cm^{-1}) modes.

We see also that the time required for the systems to recover its equilibrium H-bond structure is ~1 ps, a time similar to that obtained in our previous studies on the $HOD/D_2O_{(l)}$[44] system (~1.2 ps at 295 K) and $H_2O_{(l)}$[46] (~0.8 at 295 K). This result agrees well with the experimental analysis by Schwarzer *et al.*,[22] which concluded that the energy is transferred into nuclear degrees of freedom of the solvent, leading to a rearrangement of the hydrogen bond network within 0.9 ps. Tokmakoff *et al.*[31] determined that the time scales for H-bond rearrangements decrease from roughly 2 ps at 278 K to 0.5 ps at 345 K in the $HOD/H_2O_{(l)}$ system, with these values therefore being fully compatible with the results from the MDQT simulations.

IV. CONCLUSIONS

In this paper we have studied the vibrational relaxation of the OD stretching mode of HOD in liquid H_2O water at 303 K using the molecular dynamics with quantum transitions method. In these simulations, both the OD stretching and the overtone bending modes of the solute molecule, as well as the solute and solvent bending vibrations, are treated quantum mechanically, while the translational and rotational degrees of freedom are described classically.

In order to analyze the influence of the vibrational energy gaps on the channels during the relaxation process, we have prepared a new version of the Ferguson[62] SPC/E potential, referred to as the SPC/EM potential, which provides vibrational frequencies in solution closer to the experimental values. The relaxation times obtained in this work for the OD stretching are in satisfactory agreement with experiments.

By following the vibrational hops, it is shown that the energy transfer into the rotational degrees of freedom is favored with respect to the transfer into the translational ones. This energy transfer significantly alters the H-bond network around the HOD molecule. Thus, the average number of hydrogen bonds decreases from 3.80 to 3.55, and the system requires ~1 ps to recover its equilibrium H-bond structure.

The analysis of the hops between vibrational levels during the dynamic reveals that the relaxation of the OD mode involves a complex mechanism with different competing channels. Most of the molecules relax through a IVR process, although the presence of an intermolecular channel involving the excitation of the δ_{H_2O} bending mode of the solvent molecules is significant. Of the intramolecular channels, the most important corresponds to the δ_{HOD} bending mode, but there is also a significant contribution corresponding to the direct relaxation to the ground state. The participation of the $\delta^2_{H_2O}$ overtone is also evaluated, but its contribution is comparatively minor when the energy gaps are simulated using the SPC/EM potential. The proposed mechanism supposes a compromise between the different interpretations of the experimental measurements proposed in recent years for the description of the vibrational relaxation of this system.

ACKNOWLEDGMENTS

This work was partially supported by the Spanish Ministerio de Economía y Competitividad under Project Nos. CTQ2016-79345-P and CONSOLIDER CSD2009-00038 and by the Fundación Séneca del Centro de Coordinación de la Investigación de la Región de Murcia under Project No. 19419/PI/14-2.

[1] H. J. Bakker, H. Nienhuys, G. Gallot, N. Lascoux, G. Gale, J. C. Leicknam, and S. Bratos, J. Chem. Phys. **116**, 2592 (2002).
[2] A. J. Lock and H. J. Bakker, J. Chem. Phys. **117**, 1708 (2002).
[3] R. Laenen, K. Simeonidis, and A. Laubereau, J. Phys. Chem. B **106**, 408 (2002).
[4] A. Pakoulev, Z. Wang, and D. D. Dlott, Chem. Phys. Lett. **371**, 594 (2003).
[5] Z. Wang, A. Pakoulev, Y. Pang, and D. D. Dlott, Chem. Phys. Lett. **378**, 281 (2003).
[6] H. J. Bakker, A. J. Lock, and D. Madsen, Chem. Phys. Lett. **384**, 236 (2004).
[7] H. J. Bakker, A. J. Lock, and D. Madsen, Chem. Phys. Lett. **385**, 329 (2004).
[8] A. Pakoulev, Z. Wang, Y. Pang, and D. D. Dlott, Chem. Phys. Lett. **385**, 332 (2004).
[9] E. T. J. Nibbering and T. Elsaesser, Chem. Rev. **104**, 1887 (2004).
[10] R. Rey, K. B. Moller, and J. T. Hynes, Chem. Rev. **104**, 1915 (2004).
[11] Z. Wang, Y. Yoonsoo, and D. D. Dlott, Chem. Phys. Lett. **397**, 40 (2004).
[12] T. Steinel, J. B. Asbury, J. Zheng, and M. D. Fayer, J. Phys. Chem. A **108**, 10957 (2004).
[13] J. B. Asbury, T. Steinel, K. Kwak, S. A. Corcelli, C. P. Lawrence, J. L. Skinner, and M. D. Fayer, J. Chem. Phys. **121**, 12431 (2004).
[14] Z. Wang, A. Pakoulev, Y. Yoonsoo, and D. D. Dlott, J. Phys. Chem. **108**, 9054 (2004).
[15] J. J. Loparo, C. J. Fecko, J. D. Evans, S. T. Roberts, and A. Tokmakoff, Phys. Rev. B **70**, 180201 (2004).
[16] O. F. A. Larsen and S. Woutersen, J. Chem. Phys. **121**, 12143 (2004).
[17] P. Bodis, O. F. A. Larsen, and S. Woutersen, J. Phys. Chem. A **109**, 5303 (2005).
[18] N. Huse, S. Ashihara, E. T. J. Nibbering, and T. Elsaesser, Chem. Phys. Lett. **404**, 389 (2005).
[19] C. J. Fecko, J. J. Loparo, S. T. Roberts, and A. Tokmakoff, J. Chem. Phys. **122**, 054506 (2005).
[20] M. L. Cowan, B. D. Bruner, N. Huse, J. R. Dwyer, B. Chugh, E. T. J. Nibbering, T. Elsaeser, and R. J. D. Miller, Nature **434**, 199 (2005).
[21] A. M. Dokter, S. Woutersen, and H. J. Bakker, Phys. Rev. Lett. **94**, 178301 (2005).
[22] D. Schwarzer, J. Lindner, and P. Vöhringer, J. Chem. Phys. **123**, 161105 (2005).
[23] D. Schwarzer, J. Lindner, and P. Vöhringer, J. Phys. Chem. A **110**, 2858 (2006).
[24] S. Ashihara, N. Huse, A. Espagne, E. T. J. Nibbering, and T. Elsaesser, Chem. Phys. Lett. **424**, 66 (2006).
[25] J. Lindner, P. Vöhringer, M. S. Pshenichnikow, D. Cringus, D. A. Wiersma, and M. Mostovoy, Chem. Phys. Lett. **421**, 329 (2006).
[26] J. Lindner, D. Cringus, M. S. Pshenichnikow, and P. Vöhringer, Chem. Phys. **341**, 326 (2007).
[27] S. Ashihara, N. Huse, A. Espagne, E. T. J. Nibbering, and T. Elsaesser, J. Phys. Chem. A **111**, 743 (2007).
[28] Z. Wang, Y. Pang, and D. D. Dlott, J. Phys. Chem. A **111**, 3196 (2007).
[29] T. Schäfer, J. Lindner, P. Vöhringer, and D. Schwarzer, J. Chem. Phys. **130**, 224502 (2009).
[30] K. Tielrooij, C. Petersen, Y. Rezus, and H. Bakker, Chem. Phys. Lett. **471**, 71 (2009).
[31] R. Nicodemus, K. Ramasesha, S. Roberts, and A. Tokmakoff, J. Phys. Chem. Lett. **1**, 1068 (2010).
[32] S. Ashihara, S. Fujioka, and K. Shibuya, Chem. Phys. Lett. **502**, 57 (2011).
[33] J. Deak, S. T. Rhea, L. K. Iwaki, and D. D. Dlott, J. Phys. Chem. A **104**, 4866 (2000).

[34]F. Ingrosso, R. Rey, T. Elsaesser, and J. T. Hynes, J. Phys. Chem. A **113**, 6657 (2009).
[35]H. K. Nienhuys, S. Woutersen, R. A. van Santen, and H. J. Bakker, J. Chem. Phys. **111**, 1494 (1999).
[36]W. J. Smit and H. J. Bakker, J. Chem. Phys. **139**, 204504 (2013).
[37]R. Nicodemus, S. Corcelli, J. Skinner, and A. Tokmakoff, J. Phys. Chem. B **115**, 5604 (2011).
[38]F. Perakis and P. Hamm, J. Phys. Chem. B **115**, 5289 (2011).
[39]J. Jeon, J. H. Lim, S. Kim, H. Kim, and M. Cho, J. Phys. Chem. A **119**, 5356 (2015).
[40]G. Tian, Chem. Phys. **328**, 216 (2006).
[41]A. Bastida, J. Zúñiga, A. Requena, I. Sola, N. Halberstadt, and J. A. Beswick, Chem. Phys. Lett. **280**, 185 (1997).
[42]A. Bastida, J. Zúñiga, A. Requena, N. Halberstadt, and J. A. Beswick, J. Chem. Phys. **109**, 6320 (1998).
[43]A. Bastida, C. Cruz, J. Zúñiga, A. Requena, and B. Miguel, J. Chem. Phys. **121**, 10611 (2004).
[44]A. Bastida, J. Zúñiga, A. Requena, and B. Miguel, J. Chem. Phys. **136**, 234507 (2012).
[45]A. Bastida, M. Soler, J. Zúñiga, A. Requena, A. Kalstein, and S. Fernández-Alberti, J. Phys. Chem. B **116**, 2969 (2012).
[46]B. Miguel, J. Zúñiga, A. Requena, and A. Bastida, J. Phys. Chem. B **118**, 9427 (2014).
[47]J. C. Tully, J. Chem. Phys. **93**, 1061 (1990).
[48]S. Hames-Schiffer and J. C. Tully, J. Chem. Phys. **101**, 4657 (1994).
[49]N. Makri, Annu. Rev. Phys. Chem. **50**, 167 (1999).
[50]J. C. Tully, Faraday Discuss. **110**, 407 (1998).
[51]M. D. Hack and D. G. Truhlar, J. Phys. Chem. A **104**, 7917 (2000).
[52]J. C. Tully, in *Modern Methods for Multidimensional Dynamics Computations in Chemistry*, edited by D. L. Thompson (World Scientific, 1998), pp. 34–72.
[53]S. Okazaki, Adv. Chem. Phys. **118**, 191 (2001).
[54]S. Hammes-Schiffer and S. R. Billeter, Int. Rev. Phys. Chem. **20**, 591 (2001).
[55]K. Drukker, J. Comput. Phys. **153**, 225 (1999).
[56]G. Worth and M. Robb, in *The Role of Degenerate States in Chemistry: A Special Volume of Advances in Chemical Physics*, edited by M. Baer and G. Billing (John Wiley and Sons, Inc., 2002), pp. 355–431.
[57]J. C. Tully, Int. J. Quantum Chem. **S25**, 299 (1991).
[58]M. F. Herman, J. Chem. Phys. **81**, 754 (1984).
[59]M. P. Allen and D. J. Tildesley (Oxford Science Publications, Oxford, 1987).
[60]M. Svanberg, Mol. Phys. **92**, 1085 (1997).
[61]H. J. C. Berendsen, J. P. M. Postma, W. F. van Gunsteren, A. DiNola, and J. R. Haak, J. Chem. Phys. **81**, 3684 (1984).
[62]D. M. Ferguson, J. Comput. Chem. **16**, 501 (1995).
[63]J. C. Tully and R. K. Preston, J. Chem. Phys. **55**, 562 (1971).
[64]C. J. Fecko, J. D. Evans, J. J. Loparo, A. Tokmakoff, and P. L. Geissler, Science **301**, 1698 (2003).
[65]A. Bastida, J. Zúñiga, A. Requena, and B. Miguel, J. Chem. Phys. **131**, 204505 (2009).
[66]A. Kandratsenka, J. Schroeder, D. Schwarzer, and V. S. Vikhrenko, J. Chem. Phys. **130**, 174507 (2009).
[67]R. Kumar, J. R. Schmidt, and J. L. Skinner, J. Chem. Phys. **126**, 204107 (2007).